HHS Public Access

Author manuscript

J Orthop Res. Author manuscript; available in PMC 2024 October 01.

Published in final edited form as:

J Orthop Res. 2023 October ; 41(10): 2305–2314. doi:10.1002/jor.25659.

LACK OF SKELETAL MUSCLE CONTRACTION DISRUPTS FIBROUS TISSUE MORPHOGENESIS IN THE DEVELOPING MURINE KNEE

T.K. Tsinman[1,2], **Y. Huang**[3], **S. Ahmed**[3], **A.L. Levillain**[3], **MK. Evans**[1,2], **X. Jiang**[1], **N.C. Nowlan**[3,4,5], **N.A. Dyment**[*,1,2], **R.L. Mauck**[*,1,2,6]

[1]McKay Orthopaedic Research Laboratory, Department of Orthopaedic Surgery, University of Pennsylvania, Philadelphia, PA

[2]Department of Bioengineering, University of Pennsylvania, Philadelphia, PA

[3]Department of Bioengineering, Imperial College London, London, UK

[4]School of Mechanical and Materials Engineering, University College Dublin, Dublin, Ireland

[5]UCD Conway Institute, University College Dublin, Dublin, Ireland

[6]Translational Musculoskeletal Research Center, Corporal Michael Crescenz VA Medical Center, Philadelphia, PA

Abstract

Externally applied forces, such as those generated through skeletal muscle contraction, are important to embryonic joint formation, and their loss can result in gross morphologic defects including joint fusion. While the absence of muscle contraction in the developing chick embryo leads to dissociation of dense connective tissue structures of the knee and ultimately joint fusion, the central knee joint cavitates whereas the patellofemoral joint does not in murine models lacking skeletal muscle contraction, suggesting a milder phenotype. These differential results suggest that muscle contraction may not have as prominent a role in the growth and development of dense connective tissues of the knee. To explore this question, we investigated the formation of the menisci, tendon, and ligaments of the developing knee in two murine models that lack muscle contraction. We found that while the knee joint does cavitate, there were multiple abnormalities in the menisci, patellar tendon, and cruciate ligaments. The initial cellular condensation of the menisci was disrupted and dissociation was observed at later embryonic stages. The initial cell condensation of the tendon and ligaments were less affected than the meniscus, but these tissues contained cells with hyper-elongated nuclei and displayed diminished growth. Interestingly, lack of muscle contraction led to the formation of an ectopic ligamentous structure in the anterior

[*]**Corresponding authors:** Nathaniel A. Dyment, Ph.D., Assistant Professor of Orthopaedic Surgery and Bioengineering, McKay Orthopaedic Research Laboratory, Department of Orthopaedic Surgery, University of Pennsylvania, 330A Stemmler Hall, 3450 Hamilton Walk Philadelphia, PA 19104-6081, dyment@pennmedicine.upenn.edu, Robert L. Mauck, Ph.D., Mary Black Ralston Professor of Orthopaedic Surgery and Professor of Bioengineering, McKay Orthopaedic Research Laboratory, Department of Orthopaedic Surgery and Bioengineering, University of Pennsylvania, 308A Stemmler Hall, 3450 Hamilton Walk Philadelphia, PA 19104-6081, lemauck@pennmedicine.upenn.edu.

Author Contributions Statement: TKT, YH, SA, LLL, NCN, NAD, RLM contributed to the research design. TKT, YH, SA, LLL, MKE, XJ acquired and/or analyzed the data. All authors drafted and/or critically revised the paper and approved its final version.

region of the joint as well. These results indicate that muscle forces are essential for the continued growth and maturation of these structures during this embryonic period.

Keywords

knee joint; muscle contraction; meniscus; tendon; ligament

Introduction

Morphology and positioning of the patellar tendon, cruciate ligaments, and menisci are critical for the load bearing function of the knee. Shape and organization of these fibrous elements are established during embryonic joint formation, during which time cells are specified and patterned within the hindlimb cartilage anlagen and emerge as distinct structures following joint cavitation[1–5]. Interestingly, key stages of joint development are coincident with initiation of skeletal muscle contraction, and while the body weight bearing function of the knee does not become prominent until after birth, embryonic knee joints experience considerable mechanical perturbations as a result of passive and active (i.e., skeletal muscle contraction) fetal movements [6–11]. Postnatally, the magnitude and direction of forces placed on these tissues (as a result of muscle contraction and weight bearing) are thought to govern further tissue functional maturation, homeostasis, and degeneration. However, the precise role of muscle loading during the earliest events of intra-articular fibrous tissue formation are not fully explored.

Decades of work have established that skeletal muscle contraction is a key regulator of joint morphogenesis as a whole[12–17]. The loss of muscle forces has varied effects on joint development, depending on the species and joint type. In the chick, induced skeletal muscle paralysis has been reported to lead to the fusion of the majority of articulating joints and causes gross morphologic defects within the spine [10,13,14,18]. With a specific focus on the knee joint, Mikic *et al.* also demonstrated that abrogation of muscle contraction (through *in ovo* small molecule inhibition) did not block the initial stages of knee meniscus formation, but did result in eventual dissociation of the meniscus which progressed to joint fusion at later stages of embryonic growth[10]. This result was one of the first to demonstrate that muscle-derived forces are necessary to maintain cellular condensation necessary for knee meniscus morphogenesis. In addition to work in chick, genetic mouse models have enabled the investigation of the effects of embryonic muscle contraction on the development of mammalian joints. In particular, Splotch-delayed (*Spd*) mice, in which skeletal muscle in the limbs fails to develop, and Muscle Dysgenesis (*mdg*) models, in which muscles form but are non-contractile, display some of the same phenotypes that have been described in the muscle-paralysis avian models. Yet, several differences between these murine muscle mutants and avian models have emerged. Most notably, while some articulating joints in the appendicular skeleton of muscle mutant mice failed to undergo cavitation and fused [12,19], the knee joint showed few overt changes aside from lack of cavitation of the patellofemoral joint [12,14,20–22].

This discrepancy in the knee joint phenotypes between chick and mouse studies has called into question whether muscle contraction is required for knee joint specification and maturation. However, these conclusions are largely derived from macroscale assessment of the joint and its overall morphology of the resultant joint. Notably, the knee contains intra-articular ligamentous and fibrocartilaginous tissues (e.g., cruciate ligaments and the menisci) that distinguish it from other diarthrodial joints, and previous studies did not query the role of muscle contraction on the development of these unique tissues at high resolution. To address this, we used multiaxial cryohistology and high-resolution imaging to rigorously evaluate the progression of murine knee joint development in muscular dysgenesis (*mdg*) and splotch delayed (*Spd*) mouse lines, with a focus on the dense connective tissues of the knee joint (Figure 1). We observed striking yet distinct deficits in the embryonic formation and growth of the menisci and cruciates, along with aberrant tissue formation, demonstrating that the establishment of these soft tissues in the murine joint is sensitive to the presence of muscle contraction forces.

Methods

Animals:

All mouse work was done in accordance with European legislation (Directive 2010/63/EU). Heterozygous Splotch-delayed ($Pax3^{spd/+}$) males and females were obtained from the Jackson Laboratory (RRID: IMSR_JAX:000565) and crossed to produce homozygous $Pax3^{spd/spd}$ '*Spd*' muscleless embryos [23]. The muscular dysgenesis (*mdg*) line, in which skeletal muscle forms but is non-contractile [21], was obtained from E. Zelzer (Weizmann Institute, Israel). Heterozygous females and males were mated to provide litters containing *mdg* homozygous embryos. Based on previous work characterizing muscle mutant strain phenotypes, both heterozygous and wildtype littermates were used as controls in this study and are referred to as WT [12,23,24]. Embryonic hindlimbs were harvested at Theiler Stage (TS) TS24 (corresponding to E15.5) and TS27 (corresponding to E17.5) from the *mdg* line, as well as TS27 samples from the *Spd* line and stored either in 70% ethanol or embedded directly in OCT, and stored at −80°C. For each strain and timepoint, 3 animals from multiple litters were analyzed.

Tissue sectioning:

Samples in ethanol were rehydrated and OCT samples were washed in PBS. Samples were then fixed in 4% PFA for 2 days at 4°C, transferred to PBS, and shipped on ice from the UK to University of Pennsylvania. Upon arrival, samples were transferred to 30% sucrose, maintained at 4°C overnight, and subsequently embedded in OCT. Knee joints were serially cryo-sectioned in the coronal or sagittal planes using cryofilm 2C (Section-lab Co), at a thickness of 8μm or 20μm (Dyment *et al.*, 2016). Care was taken to ensure proper alignment of the joint during sectioning such that similar anatomical locations were analyzed and compared between samples.

Fluorescent tissue staining and imaging:

Film-stabilized 8μm tissue sections were fixed to glass slides using chitosan adhesive. For gross knee morphology, cell quantification, and nuclear shape analysis, sections were

rehydrated, permeabilized with 0.1% Triton-X (Millipore Sigma, T8787) in PBS for 1hr and stained with Alexa-Fluor Phalloidin (Invitrogen, Cat#: A12379, A12381) at 1:800 in 1% BSA overnight at 4°C. Samples were counterstained with 1:800 Hoechst 33342 (Life Technologies, H3570) and imaged using the Zeiss Axio Scan.Z1 slide scanner (20X objective, Colibri 7 LED illumination source). Representative sample sections were also imaged throughout their depth via Nikon A1R confocal system (10X, 1024×1024px, 1.24μm/pixel (px), 1μm step size). For nuclear shape analysis, confocal z-stacks (0.2μm step size) of nuclei (DAPI) were acquired (60X objective, 1024×1024px, 0.04μm/px) throughout the section thickness.

Second harmonic generation (SHG) imaging:

Collagen fibers of unstained 20μm TS27 sagittal sections were visualized via forward scatter second harmonic generation (SHG) imaging using a Leica SP8 2-Photon Microscope with a 20X water immersion objective (laser wavelength: 890nm). Z-stacks (1μm step size) were acquired throughout the depth of the tissue. Laser intensity and gain was kept constant between samples. Full fields of view for tissue sections were first acquired at 0.75X zoom (1024×1024px, 0.72μm/px), after which regions within tissues of interest (patellar tendon, ACL, etc.) were further imaged at 7X zoom (1024×1024px, 0.07μm/px). Maximum intensity projections of z-stacks are shown.

Image visualization and analysis:

All image processing was performed using Fiji [25]. For representative images, maximum intensity projections were generated from acquired z-stacks. To determine cellularity of meniscal condensation in developing knee joints, the polygon selection tool was used to segment the meniscus boundary and remove any other tissue from the field of view. The nuclei were then identified via intensity thresholding, watershedding, and masking for each image. The ‘analyze particles’ function was then used to count cells in each section. Cell numbers from three sections per animal were counted and the average was reported, with no two sections adjacent to one another in a series of serial sections, to avoid analysis of the same cells. 3 biological replicates per genotype and timepoint were analyzed. For nuclear aspect ratio measurements, individual nuclei of 60X confocal z-stacks were manually segmented in each z-slice from the adjacent nuclei using the polygon tool. A maximum intensity projection of an individual nucleus’ z-stack was made, and the nuclear shape was determined through the ‘analyze particles’ function. The aspect ratio (‘AR’) output metric is reported in the analysis. Measurements for individual nuclei were pooled between two biological replicates per tissue with a total of n>50 nuclei. All plotting was done using custom R scripts and the ‘ggplot2’ package as well as GraphPad Prism software.

Statistical analysis:

For meniscus cell number counts, groups were compared using a two-tailed Student’s t-test ($p<0.05$ cut-off). For nuclear elongation measurements, groups were compared by Kruskal Wallis Test followed by a Dunn Test for pairwise comparisons (Bonferroni p-adjustment method, $p<0.05$ cut-off).

Results

Loss of muscle contraction reduces meniscus size and persistence

We first evaluated both the medial and lateral menisci in the *mdg* mouse line, which develops with non-contractile skeletal muscle. At TS24 (E15.5), the knee joint was cavitated in both control and *mdg* mutant samples, apart from the patellofemoral joint that did not cavitate (Figure S1), as previously reported [20]. These findings confirmed that, unlike many articulating joints, knee joint cavitation still occurs in the absence of muscle contraction[12,20]. However, a closer examination at the forming knee menisci revealed that, while wild-type (WT) embryos contained wedge-shaped cellular condensates in areas corresponding to the medial and lateral menisci, the size of these condensates in *mdg* samples was reduced with a corresponding reduction in cell number (Figure 2b, c). These smaller condensates were not due to smaller joint sizes overall, as the width of the tibial plateau was not significantly different in the *mdg* mice compared to WT littermates (Figure 2d). With further developmental progression at TS27, WT menisci continued to organize and compact, with distinct cell-rich structures clearly visible. At this same time point, *mdg* mutant littermates exhibited signs of dissociation, with marked reduction in cell number within the presumptive meniscal region and oftentimes a lack of a clear tissue boundary (Figure 2b, c).

Interestingly, deficits in meniscus condensation in the absence of muscle contraction varied depending on anterior-to-posterior location. In the anterior horn, the meniscus was completely dissociated by TS27, and no fibrous insertion to the tibial plateau was detected (Figure 2e, Figure S2). Conversely, the posterior horns were fully formed and attached to the tibial plateau through fibrous insertions, although they were visibly diminished in size. Finally, we also observed a loss of curvature of both the femoral and tibial surfaces in muscle mutant knees (Figure 3), which was noted previously [17,19]. This flattening of the surfaces is reminiscent of a meniscus deficient knee in humans [26]. Taken together, differences in meniscus formation within the *mdg* knee joints was discernable at the time of joint cavitation (TS24) and became progressively worse with further development (TS27). These findings (location-dependent differences in meniscus condensation deficits, femoral/tibial flattening) were also present in the TS27 joints of *Spd* mice, a mutant strain that completely lacks skeletal muscle in the limb (Figure 3).

Loss of muscle contraction results in patellar tendon and cruciate ligament abnormalities and the emergence of an ectopic ligamentous tissue.

Given the marked changes in meniscus condensation in muscle mutants, we also evaluated changes in the cruciate ligaments (ACL and PCL) and the patellar tendon (PT) of these animals. Muscle contraction did not have an impact on the anatomical positioning of the ACL, PCL, or PT, except for the previously reported fusion of the patella to the femur [20]. Each tissue contained linear arrays of cells with fibrillar actin organization in both WT and *mdg* joints at TS24 (Figure 4a,b). Surprisingly, TS24 *mdg* joints also contained an additional ligamentous structure, attached to the femur and tibia in the anterior compartment between the PT and the anterior insertions of the ACL and PCL (Figure 4a, yellow arrowhead). This structure, which was observed in all mutant samples, appeared to be an ectopic ligament-like tissue, as it exhibited similar cellular patterning as the endogenous fibrous structures (Figure

4b). Although ligamentous tissues of TS24 *mdg* joints seemed to have proper positioning (PT and cruciates) and alignment (PT, cruciates, ectopic ligament), resident cells of these tissues had abnormally shaped and hyper-elongated nuclei (as measured by nuclear aspect ratio, NAR) (Figure 4c,d).

In addition to the apparent dissociation of the anterior region of the medial meniscus in the *mdg* limbs at TS27, the PT, cruciates, and the ectopic ligament-like structure were still present but displayed abnormalities in tissue structure and cell morphology (Figure 5a). The difference in nuclear elongation between cells of WT and *mdg* tissues was not as marked at this later developmental time point, as highlighted by NAR measurements within the TS27 PT and ectopic ligamentous tissue. However, mutant tissues continued to have a subpopulation of resident cells with abnormally elongated nuclei (Figure 5b, Figure S3).

Though the PT and cruciates appeared reduced in size by TS27, all mutant tissues contained aligned fibrillar collagen and organized attachments to the adjoining cartilage (Figure 5c, Figure S4a). However, SHG signal intensity and density were reduced in the mutants. Importantly, all changes noted in the ligamentous tissue of *mdg* mutants, including the formation of the ectopic ligamentous tissue, were similar in the *Spd* mutant mice at TS27 (Figure S4b,c). The fact that knee joint fibrous tissue changes were consistent between two independent mouse lines that lack skeletal muscle contraction suggest that exogenous mechanical forces play a role in the continued growth and maturation of these knee joint tissues.

Discussion

This work demonstrates the impact of muscle contraction on developing murine knee joint fibrous tissues, providing further evidence for regulation of fibrous tissue morphogenesis by extrinsic mechanical forces. In the meniscus, loss of muscle forces in *mdg* mutants resulted in cellular condensations that were significantly diminished at the joint cavitation stage (TS24). While this provides evidence that muscle contraction is critical for normal meniscus tissue formation, it is unclear whether this is a result of impaired initiation of cellular condensation and patterning, or if this is indicative of progressive failure to maintain the condensed state in the absence of external mechanical stimuli, or both (Figure 6a). The continued reduction in size of meniscal condensates by TS27 indicates the importance of muscle contraction to tissue growth and maturation (Figure 2, Figure S2), but additional biochemical and molecular analyses specifically investigating the mechanisms for this reduced growth are needed. Additionally, progressive loss of meniscus structures was coincident with flattening of the femoral and tibial surfaces (Figure 3). Strikingly, such changes often occur in humans as a consequence of meniscectomy (i.e., Fairbank's changes) and indicate aberrant joint remodeling in response to meniscus insufficiency [26,27]. These parallels suggest that, in both embryonic as well as mature tissues, the curvature of the articulating surfaces depends on the integrity of the meniscus structure, underscoring the reciprocity between adjacent tissues in establishing the proper shape critical to their function.

As previously reported (and unlike other joints), we confirm here that muscle contraction forces are not required for knee joint cavitation, except for the patellofemoral joint [12,17,20]. However, these cues are instrumental in the proper formation of the intra-articular fibrous structures that distinguish the knee joint from its diarthrodial counterparts. Importantly, meniscus dissociation following knee joint cavitation in *mdg* and *Spd* skeletal muscle mouse mutant strains phenocopied what is seen during pharmacologic paralysis of embryonic chick muscles *in ovo* [10]. This confirms the integral role of muscle contraction forces in development in both the murine and avian models. It should be noted, however, that discrepancies between the two models do exist. For example, while numerous *in ovo* paralysis studies have shown progressive fusion of the knee joint following meniscus dissociation, *mdg* and *Spd* knees remained fully cavitated even at TS27, when the meniscus structures were almost completely gone [28–35]. It is intriguing to consider to what extent the variation in phenotypes observed in avian and mouse models of embryonic muscle contraction perturbation is due to the differences between the *in ovo* (external) versus *in utero* (internal) developmental environment. Our findings in a mammalian system not only confirm the critical role of muscle forces for *in utero* meniscus development, but also build upon existing literature in chick by showing that the loss of the meniscus is asymmetric. Analysis of serial cryosections demonstrated that an absence of muscle contraction resulted in a more severe phenotype in the anterior aspects of the joint (Figure 3, Figure S2). This suggests that factors that direct or support meniscus morphogenesis may vary based on anterior-to-posterior location. It is possible that passive embryonic motion, or a higher degree of impingement due to knee flexion *in utero* [36], provide sufficient physical cues that partially mitigate the impact of the loss of muscle generated forces in the posterior, but not anterior, segment of the joint space. Moreover, in addition to the absence of the anterior meniscal horn, we noted the lack of the associated ligamentous insertion of the meniscus anterior horn into the tibial plateau in muscle mutants. This lack of meniscal attachment suggests that, at the critical time of meniscus formation and early growth (TS24-TS27), mutant tissues fail to form important boundary constraints that may further contribute to some of the observed changes in menisci from these mutant mice.

Examination of the patellar tendon (PT) and cruciate ligaments of the knee also revealed that loss of muscle contraction caused a disruption in the development of these intra-articular structures (Figure 6b). Specifically, the initial assembly and alignment of cells into linear arrays was not significantly impacted by the lack of muscle contraction (Figure 4). These cells also generated a nascent fibrillar collagen network by TS27, albeit reduced in size compared to littermate control tissues (Figure 5, Figure S4). However, cell nuclei within TS24 *mdg* PT and ACL tissues (Figure 4d) were hyper elongated compared to WT littermates. Such elongation could arise due to increased resident cell contractility (deformation through cytoskeletal tension and nuclear engagement) or via a heightened level of tissue pre-stress (extrinsic tensioning of the aligned cell mass) due to the lack of certain cues typically provided by joint motion. The notable cellular hyper-elongation may thus suggest that a requirement for the proper patterning of knee joint tendons and ligaments is achieving a certain tension threshold that, in embryos with functional muscle, is achieved through a balance of cell generated forces and external forces from muscle contraction.

This concept of reciprocity between cell-generated and extrinsic mechanical forces is supported by *in vitro* studies showing that cells within fibrous tissues can sense both increases and decreases in externally applied tension. For instance, when a sharp drop in tension occurs, cells activate a catabolic program resulting in matrix remodeling [37,38] and in certain cases can activate their non-muscle myosin mediated contractile machinery to correct the overall tension back to homeostatic levels [39]. Similarly, in cell constructs, changes in external tension are sensed, and coordinately contracted against, by the collective cell population [40]. Thus, loss of muscle contraction could cause a decrease in nascent tension that the patterned cells attempt to correct by collectively contracting—leading to the observed hyper-elongated state (Figure 4). Furthermore, *in vitro* models of cell-rich linear constructs grown in the presence of boundary constraints demonstrate that an imbalance in stiffness of the extracellular matrix with the active contractility of resident cells can result in 'necking' of the cell-matrix material, leading to tissue failure through narrowing and elongation [41]. While we did not observe fully failed tissues in the joints, tendons and ligaments in both *mdg* and *Spd* mutants appeared greatly reduced in size by the later stage of development, and the matrix was not as dense or abundant (as observed by SHG) compared to littermate controls (Figure 5, Figure S4). Thus, in a scenario where muscle forces are absent, cells may be able to sense the improper tensioning and attempt to compensate through hypercontractility—subsequently leading to cell shearing and microdamage of the nascent matrix (Figure 6b).

Unexpectedly, we observed the formation of an ectopic ligamentous structure within the anterior portion of the joint capsule, attached to both the femur and tibia anterior to the cruciate attachments in both *mdg* and *Spd* lines (Figure 3). This tissue appeared to pattern and grow much like the endogenous knee ligaments – via initial assembly and elongation of the resident cells into a linear shape, followed by the appearance of linearly aligned fibrillar collagen matrix (Figure 4a,b; Figure 5a,c). While this structure anatomically appears ligament-like, future studies are needed to determine if the cells within this structure express ligamentous markers. Though it is unclear what cell sources contribute to this aberrant tissue condensation, the robust formation of a knee ectopic ligamentous structure in the absence of muscle contraction (observed in all *mdg* and *Spd* animals used in this study) suggests that extrinsic physical cues may dictate cell fate decisions of certain knee tissues.

While this study indicates a critical role for muscle loading in knee joint growth and development, it did have limitations. The sample size and age groups were limited given that specimens came from a previous study focused on the spine of these mice [42] and so additional samples at other developmental states were not available at the time this work was being performed. However, we are currently expanding this line in our colony again and future studies will investigate the specific biomolecular mechanisms that led to the observed phenotypes, including additional time points and analyses (e.g., gene expression, immunofluorescence for matrix composition, apoptosis staining, and catabolic enzyme activity assays). Earlier time points (e.g., TS22/E13.5) are also needed to determine how the initial formation of these tissues might be impacted in the absence of muscle loading, which would elucidate the importance of muscle loading compared to other biophysical (e.g., passive tension) or biochemical cues [43].

Taken together, our results demonstrate that muscle contraction is critical for the continued growth and maintenance of all dense connective tissues in the knee joint. Why muscle contraction has a more prominent role in certain tissues, and regions within tissues, compared to others is unknown. These structures all originate from a common cell origin (i.e., the interzone) [44,45]. However, the onset and duration of certain morphogens (e.g., GDF5) contribute to differentiation of tissue-specific cell types within the knee joint [45,46]. The timing and persistence of these molecular factors, some of which are mechanoresponsive, is clearly critical for the development and maintenance of these dense connective tissues [36,47,48]. Given the differences in knee joint fibrous tissue formation in the absence of muscle forces, our work indicates that, in addition to cell origin, changing bioavailability of growth and differentiation factors, and variance in gene expression dynamics, extrinsic physical cues contribute to the continued development of distinct tissue types of the knee. Explicating how these cells spatially and temporally integrate both molecular and mechanical inputs to drive tissue formation and maturation may reveal new insights into how these unique tissues form, fail, and ultimately direct new approaches for their repair.

Supplementary Material

Refer to Web version on PubMed Central for supplementary material.

Acknowledgements

This research received funding from the National Institutes of Health (NIH R01 AR075418, P30 AR069619, R00 AR067283, P50 AR080581, and T32 AR007132 (MKE, TKT)), the Center for Engineering Mechanobiology (NSF Science and Technology Center, CMMI-1548571) and the European Research Council under the European Union's Seventh Framework Programme (ERC Grant agreement number 336306).

REFERENCES

1. Gamer LW, Xiang L, Rosen V. 2017. Formation and maturation of the murine meniscus. J. Orthop. Res. 35(8):1683–1689. [PubMed: 27664939]
2. McDermott LJ. 1943. Development of the Human Knee Joint. Arch. Surg. 46(5):705 [cited 2015 Dec 1] Available from: http://jbjs.org/content/65/4/538.abstract.
3. Haines RW. 1947. The development of joints. J. Anat. 81(Pt 1):33–55.
4. Mitrovic D. 1978. Development of the Diarthrodial Joints in the Rat Embryo. Am. J. Anat. 151:475–486. [PubMed: 645613]
5. Ratajczak W. 2000. Early development of the cruciate ligaments in staged human embryos. Folia Morphol. (Warsz). 59(4):285–290. [PubMed: 11107700]
6. Hamburger V, Balaban M, Oppenheim R, Wenger E. 1965. Periodic motility of normal and spinal chick embryos between 8 and 17 days of incubation. J. Exp. Zool. 159(1):1–13 [cited 2021 Sep 23] Available from: https://pubmed.ncbi.nlm.nih.gov/5215365/. [PubMed: 5215365]
7. Kodama N, Sekiguchi S. 1984. The development of spontaneous body movement in prenatal and perinatal mice. Dev. Psychobiol. 17(2):139–150 [cited 2021 Sep 21] Available from: https://onlinelibrary.wiley.com/doi/full/10.1002/dev.420170205. [PubMed: 6706018]
8. de Vries J, Visser G, Prechtl H. 1986. Fetal behaviour in early pregnancy. Eur. J. Obstet. Gynecol. Reprod. Biol. 21(5–6):271–276 [cited 2021 Sep 23] Available from: https://pubmed.ncbi.nlm.nih.gov/3721038/. [PubMed: 3721038]
9. Suzue T, Shinoda Y. 1999. Highly reproducible spatiotemporal patterns of mammalian embryonic movements at the developmental stage of the earliest spontaneous motility. Eur. J. Neurosci.

11(8):2697–2710 [cited 2021 Sep 23] Available from: https://onlinelibrary.wiley.com/doi/full/10.1046/j.1460-9568.1999.00686.x. [PubMed: 10457166]

10. Mikic B, Johnson TL, Chhabra AB, et al. 2000. Differential effects of embryonic immobilization on the development of fibrocartilaginous skeletal elements. J. Rehabil. Res. Dev. 37(2):127–133. [PubMed: 10850818]
11. Verbruggen SW, Kainz B, Shelmerdine SC, et al. 2018. Stresses and strains on the human fetal skeleton during development. J. R. Soc. Interface 15(138) [cited 2021 Sep 22] Available from: https://royalsocietypublishing.org/doi/abs/10.1098/rsif.2017.0593.
12. Kahn J, Shwartz Y, Blitz E, et al. 2009. Muscle Contraction Is Necessary to Maintain Joint Progenitor Cell Fate. Dev. Cell 16(5):734–743 Available from: 10.1016/j.devcel.2009.04.013. [PubMed: 19460349]
13. Rolfe RA, Bezer JH, Kim T, et al. 2017. Abnormal fetal muscle forces result in defects in spinal curvature and alterations in vertebral segmentation and shape. J. Orthop. Res. 35(10):2135–2144 [cited 2020 Sep 1] Available from: http://doi.wiley.com/10.1002/jor.23518. [PubMed: 28079273]
14. Nowlan NC, Sharpe J, Roddy KA, et al. 2010. Mechanobiology of embryonic skeletal development: Insights from animal models. Birth Defects Res. Part C - Embryo Today Rev. 90(3):203–213.
15. Rolfe R, Roddy K, Murphy P. 2013. Mechanical regulation of skeletal development. Curr. Osteoporos. Rep. 11(2):107–116. [PubMed: 23467901]
16. Felsenthal N, Zelzer E. 2017. Mechanical regulation of musculoskeletal system development. Dev. 144(23):4271–4283 [cited 2020 Sep 1] Available from: https://dev.biologists.org/content/144/23/4271.
17. Sotiriou V, Ahmed S, Nowlan NC. 2022. Recovery of skeletogenesis despite absent muscle. bioRxiv.
18. Levillain A, Rolfe RA, Huang Y, et al. 2019. Short-term foetal immobility temporarily and progressively affects chick spinal curvature and anatomy and rib development. Eur. Cells Mater. 37:23–41 [cited 2020 Sep 1] Available from: http://creativecommons.org/licenses/by-sa/4.0/.
19. Sotiriou V, Rolfe RA, Murphy P, Nowlan NC. 2019. Effects of Abnormal Muscle Forces on Prenatal Joint Morphogenesis in Mice. J. Orthop. Res. 37(11):2287–2296 [cited 2020 Sep 1] Available from: https://onlinelibrary.wiley.com/doi/abs/10.1002/jor.24415. [PubMed: 31297860]
20. Eyal S, Blitz E, Shwartz Y, et al. 2015. On the development of the patella. Development 142(10):1831–1839 Available from: http://dev.biologists.org/cgi/doi/10.1242/dev.121970. [PubMed: 25926361]
21. Pai AC. 1965. Developmental genetics of a lethal mutation, muscular dysgenesis (mdg), in the mouse: II. Developmental analysis. Dev. Biol. 11(1):93–109. [PubMed: 14300096]
22. Arvind V, Huang AH. 2017. Mechanobiology of limb musculoskeletal development. Ann. N. Y. Acad. Sci. 1409(1):18–32 [cited 2018 Jul 9] Available from: http://doi.wiley.com/10.1111/nyas.13427. [PubMed: 28833194]
23. Franz T, Kothary R, Surani M, et al. 1993. The Splotch mutation interferes with muscle development in the limbs. Anat. Embryol. (Berl). 187(2):153–160 [cited 2021 Sep 22] Available from: https://pubmed.ncbi.nlm.nih.gov/8238963/. [PubMed: 8238963]
24. Ahmed S, Rogers AV, Nowlan NC. 2022. Mechanical Loading due to Muscle Movement Regulates Establishment of the Collagen Network in the Developing Murine Skeleton. bioRxiv :2022.06.23.497302 Available from: http://biorxiv.org/content/early/2022/06/26/2022.06.23.497302.abstract.
25. Schindelin J, Arganda-Carreras I, Frise E, et al. 2012. Fiji: An open-source platform for biological-image analysis. Nat. Methods 9(7):676–682 [cited 2021 Feb 9] Available from: http://fiji.sc/Adding_Update_Sites. [PubMed: 22743772]
26. Fairbank TJ. 1948. Knee Joint Changes After Meniscectomy. J. Bone Jt. Surg. 30 B(4):664–670 [cited 2021 Aug 24] Available from: https://online.boneandjoint.org.uk/doi/abs/10.1302/0301-620X.30B4.664.
27. McDermott ID, Amis AA. 2006. The consequences of meniscectomy. J. Bone Jt. Surg. - Ser. B 88(12):1549–1556.

28. Drachman DB, Sokoloff L. 1966. The role of movement in embryonic joint development. Dev. Biol. 14(3):401–420.
29. Ruano-Gil D, Nardi-Vilardaga J, Tajedo-Mateu A. 1978. Influence of extrinsic factors on the development of the articular system. Acta Anat. 101:36–44 Available from: http://www.ncbi.nlm.nih.gov/pubmed/15237199. [PubMed: 645333]
30. Persson M 1983. The role of movements in the development of sutural and diarthrodial joints tested by long-term paralysis of chick embryos. J. Anat. 137(3):591–599. [PubMed: 6654748]
31. Bastow ER, Lamb KJ, Lewthwaite JC, et al. 2005. Selective activation of the MEK-ERK pathway is regulated by mechanical stimuli in forming joints and promotes pericellular matrix formation. J. Biol. Chem. 280(12):11749–58 [cited 2018 Apr 24] Available from: http://www.ncbi.nlm.nih.gov/pubmed/15647286. [PubMed: 15647286]
32. Osborne AC, Lamb KJ, Lewthwaite JC, et al. 2002. Short-term rigid and flaccid paralyses diminish growth of embryonic chick limbs and abrogate joint cavity formation but differentially preserve pre-cavitated joints. J. Musculoskelet. Neuronal Interact. 2(5):448–456. [PubMed: 15758413]
33. Kavanagh E, Church VL, Osborne AC, et al. 2006. Differential regulation of GDF-5 and FGF-2/4 by immobilisation in ovo exposes distinct roles in joint formation. Dev. Dyn. 235(3):826–834. [PubMed: 16425226]
34. Roddy KA, Kelly GM, van Es MH, et al. 2011. Dynamic patterns of mechanical stimulation co-localise with growth and cell proliferation during morphogenesis in the avian embryonic knee joint. J. Biomech. 44(1):143–149 Available from: 10.1016/j.jbiomech.2010.08.039. [PubMed: 20883996]
35. Singh PNP, Shea CA, Sonker SK, et al. 2018. Precise spatial restriction of BMP signaling in developing joints is perturbed upon loss of embryo movement. Development 145(5):dev153460 [cited 2018 Mar 25] Available from: http://www.ncbi.nlm.nih.gov/pubmed/29467244. [PubMed: 29467244]
36. Kim M, Koyama E, Saunders CM, et al. 2022. Synovial joint cavitation initiates with microcavities in interzone and is coupled to skeletal flexion and elongation in developing mouse embryo limbs. Biol. Open 11(6):1–13.
37. Jones DL, Daniels RN, Jiang X, et al. 2022. Mechano-epigenetic regulation of extracellular matrix homeostasis via Yap and Taz. bioRxiv :2022.07.11.499650.
38. Bonnevie ED, Gullbrand SE, Ashinsky BG, et al. 2019. Aberrant mechanosensing in injured intervertebral discs as a result of boundary-constraint disruption and residual-strain loss. Nat. Biomed. Eng. 2019 312 3(12):998–1008 [cited 2023 May 11] Available from: https://www.nature.com/articles/s41551-019-0458-4. [PubMed: 31611678]
39. Weißenbruch K, Grewe J, Hippler M, et al. 2021. Distinct roles of nonmuscle myosin II isoforms for establishing tension and elasticity during cell morphodynamics. Elife 10.
40. Holmes DF, Yeung C- YC, Garva R, et al. 2018. Synchronized mechanical oscillations at the cell-matrix interface in the formation of tensile tissue. Proc. Natl. Acad. Sci. 115(40):E9288–E9297 [cited 2018 Oct 18] Available from: www.pnas.org/cgi/doi/10.1073/pnas.1801759115. [PubMed: 30237286]
41. Wang H, Svoronos AA, Boudou T, et al. 2013. Necking and failure of constrained 3D microtissues induced by cellular tension. Proc. Natl. Acad. Sci. 110(52):20923–20928 [cited 2021 Sep 21] Available from: https://www.pnas.org/content/110/52/20923. [PubMed: 24324149]
42. Levillain A, Ahmed S, Kaimaki D, et al. 2021. Prenatal muscle forces are necessary for vertebral segmentation and disc structure, but not for notochord involution in mice. Eur. Cell. Mater. 41:558–575 [cited 2021 Aug 21] Available from: https://pubmed.ncbi.nlm.nih.gov/34021906/. [PubMed: 34021906]
43. Lipp SN, Jacobson KR, Colling HA, et al. 2023. Mechanical loading is required for initiation of extracellular matrix deposition at the developing murine myotendinous junction. Matrix Biol. 116:28–48. [PubMed: 36709857]
44. Pazin DE, Gamer LW, Cox KA, Rosen V. 2012. Molecular profiling of synovial joints: Use of microarray analysis to identify factors that direct the development of the knee and elbow. Dev. Dyn. 241(11):1816–1826 [cited 2018 Apr 16] Available from: http://doi.wiley.com/10.1002/dvdy.23861. [PubMed: 22972626]

45. Shwartz Y, Viukov S, Krief S, Zelzer E. 2016. Joint Development Involves a Continuous Influx of Gdf5-Positive Cells. Cell Rep. 15(12):2577–2587 Available from: 10.1016/j.celrep.2016.05.055. [PubMed: 27292641]

46. Hyde G, Boot-Handford RP, Wallis GA. 2008. Col2a1 lineage tracing reveals that the meniscus of the knee joint has a complex cellular origin. J. Anat. 213(5):531–538 [cited 2016 Jun 5] Available from: http://www.pubmedcentral.nih.gov/articlerender.fcgi?artid=2667547&tool=pmcentrez&rendertype=abstract. [PubMed: 19014360]

47. Tan G-K, Pryce BA, Stabio A, et al. 2020. Tgfβ signaling is critical for maintenance of the tendon cell fate. Elife 9 Available from: https://elifesciences.org/articles/52695.

48. Tan GK, Pryce BA, Stabio A, et al. 2021. Cell autonomous TGFβ signaling is essential for stem/progenitor cell recruitment into degenerative tendons. Stem Cell Reports 16(12):2942–2957 Available from: 10.1016/j.stemcr.2021.10.018. [PubMed: 34822771]

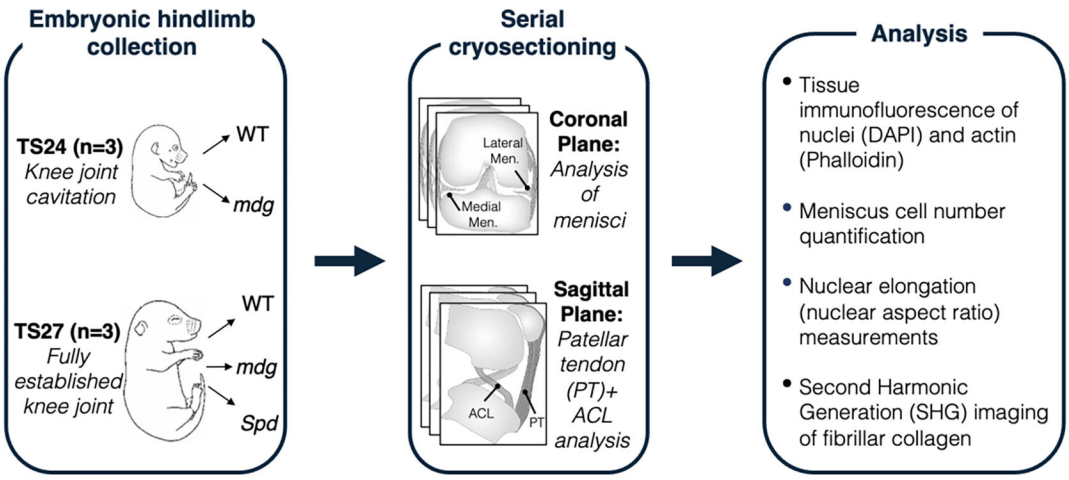

Figure 1:

Study workflow. To assess how the muscle forces impact the formation of the fibrous intra-articular tissues of the knee joint, hindlimbs were collected from wildtype (WT) and mutant (*mdg*) littermates from the Muscular Dysgenesis (*mdg*) mouse strain, wherein mutant animals develop with non-contractile skeletal muscle due to a mutation in the calcium ion channel (*Cacna1s* gene) that causes a failure in excitation-contraction coupling. Collection was done at TS24 (roughly corresponding to embryonic day E15.5 — the point of knee cavitation) and TS27 (approximately E17.5, a later stage of development in which the embryonic knee is fully formed). Additionally, for the later TS27 embryonic stage, hindlimbs from litters of the Splotch-delayed (*Spd*) mouse strain (WT and mutant), in which mutant embryos develop without any skeletal muscle, were also analyzed to compare knee joint phenotypes in two distinct mutant strains that lack joint motion from muscle contraction. Hindlimbs of all animals were serially cryosectioned in anatomical planes in which knee joint tissues of interest (meniscus, ACL, and patellar tendon) could be most robustly visualized. Cryosections were then stained, imaged via high-resolution microscopy, and tissue cellularity, nuclear shape, and fibrillar collagen content were analyzed (see methods).

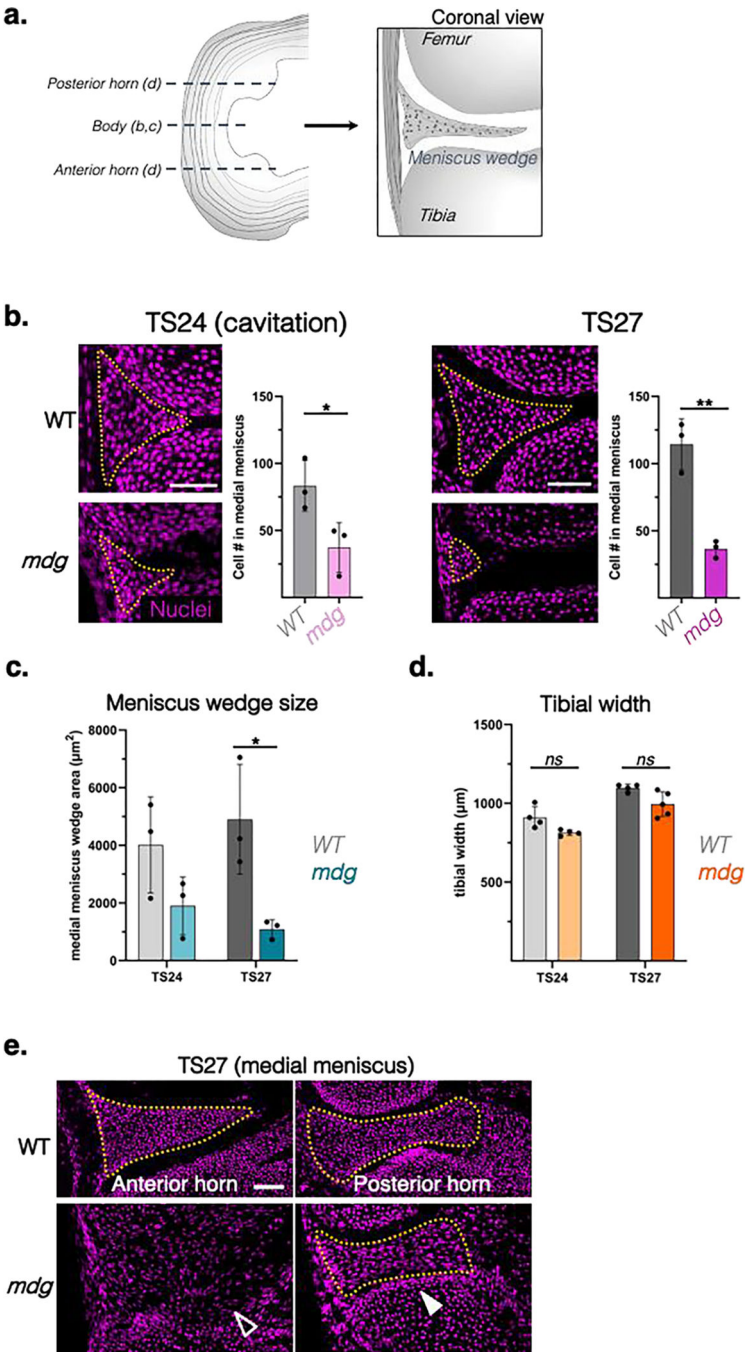

Figure 2: Alterations in meniscus morphogenesis in the absence of muscle contraction.

a) Schematic of the coronal (frontal) sections used to analyze the horn and body regions of the medial menisci in b-d. b) Representative nuclear (DAPI) stained coronal sections showing cell condensation in the meniscus body region of the developing knee at TS24 (knee joint cavitation timepoint corresponding to ~E15.5) and TS27 (~E17.5) in the muscular dysgenesis mouse (*mdg*) mouse model. Yellow dotted lines outline wedge-shaped cellular masses indicating meniscus formation in WT control and *mdg* mutant littermate joints (scale bar: 50μm). Adjacent plots show average cell number in condensates at

respective timepoints. Mean and SEM shown (n=3 animals/group). Statistical comparison by two-tailed t-test. *: $p<0.05$; **: $p<0.01$; ***: $p<0.001$. c) Quantification of cross sectional area of the body region of the medial meniscus wedge as well as the cross-sectional width of the proximal tibial head (d) of WT and *mdg* mutant tissues at TS24 and TS27. Statistical comparison of tissues at each timepoint by two-tailed t-test (*: $p<0.05$, ns: not significant). e) Representative coronal sections of the anterior medial meniscus horn (left) and the posterior horn (right) of the same meniscus in WT and *mdg* TS27 (E17.5) knee joints labeled with a nuclear stain (magenta). Yellow outlines demarcate the meniscus wedge. Note the absence of a distinct wedge-shaped condensate in the anterior horn region (empty arrowhead) compared to the condensed posterior horn wedge (white arrowhead) in the *mdg* mutant (scale bar: 50μm).

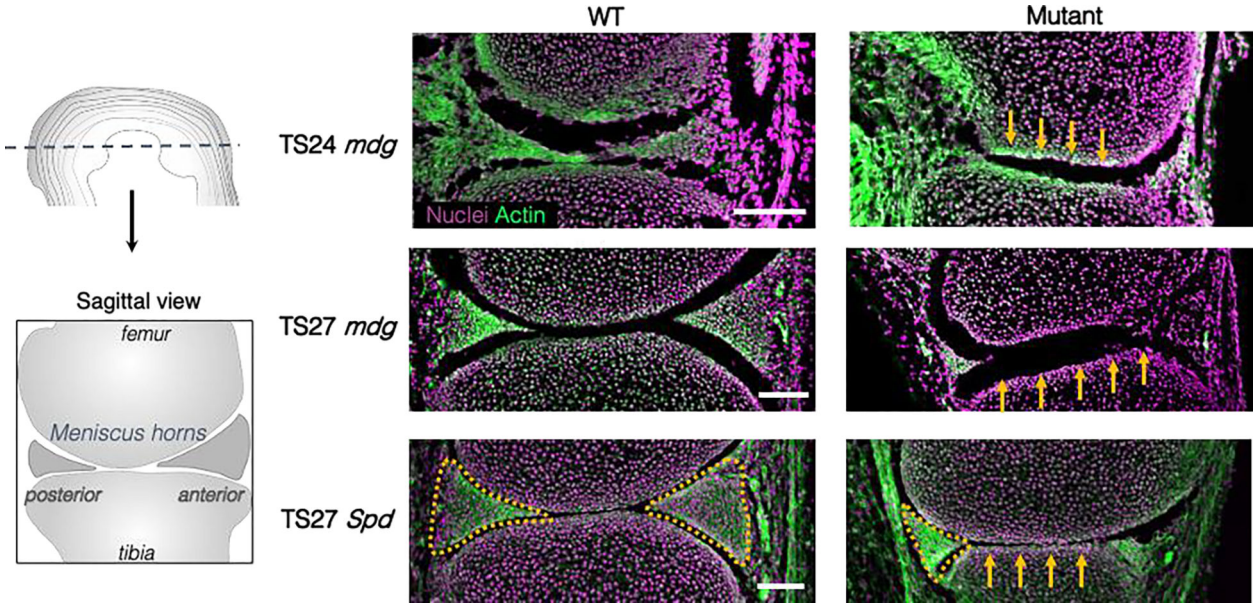

Figure 3:

Representative sagittal sections of WT (left) and either *mdg* or *Spd* mutants (right) at TS24 (E15.5) or TS27 (E17.5) stained for cell nuclei (magenta) and filamentous actin (green). *Spd* mutants lack all skeletal muscle due to a mutation in *Pax3*, resulting in hindered skeletal muscle development. Yellow arrows in mutant tissues highlight flattening of the femoral condyle and tibial plateau. Yellow outlines demarcate anterior and posterior horn wedges in the TS27 knee joints of littermates with control genotypes. Note the reduced posterior horn (yellow outline) and an absence of the anterior horn wedge in both the TS27 *mdg* and *Spd* mutants (scale bar: 100μm).

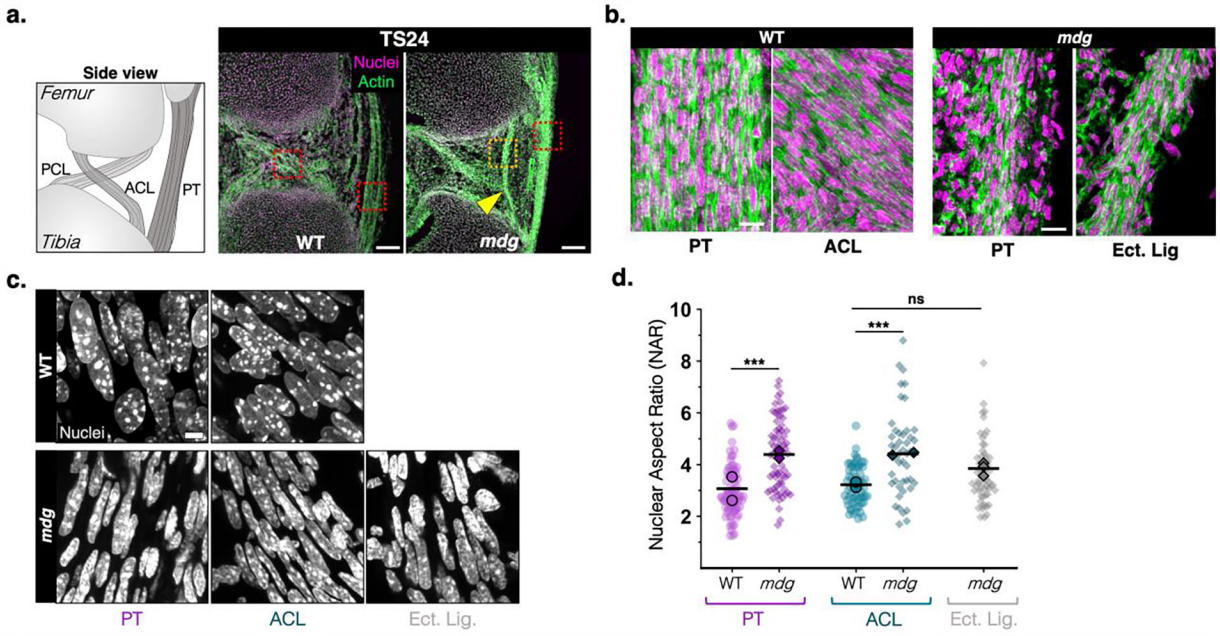

Figure 4: Abnormalities in fibrous tissue patterning and cell morphology in TS24 *mdg* knee joints.

A) Representative sagittal views of TS24 (E15.5) WT and *mdg* knee joints in the region of the cruciate ligaments and the patellar tendon, as demarcated in the schematic. PT: patellar tendon, ACL/PCL: anterior cruciate ligament/posterior cruciate ligament. Sections were stained with phalloidin (actin, green) and a nuclear counterstain (magenta). Yellow arrowhead points to ectopic ligament condensation (Ect. Lig.) in the anterior part of the joint with femoral and tibial attachments (scale bar: 100μm). b) High magnification views of regions demarcated by red and yellow boxes in a) (scale bar: 20μm). c) Representative confocal maximum projections of nuclei of resident cells of the patellar tendon, ACL, and ectopic ligament (scale bar: 5μm). d) Nuclear aspect ratio (NAR), calculated as the ratio of long to short axis of individual segmented nuclei as a metric of nuclear elongation in WT and *mdg* cells of PT, ACL, and ectopic ligaments (in *mdg* mutant knees). n>50 cells per group, taken from 2 biological replicates (mean of each replicate indicated by black symbol). Kruskal-Wallis with Dunn's Test for pairwise comparison, ***: $p<0.0001$.

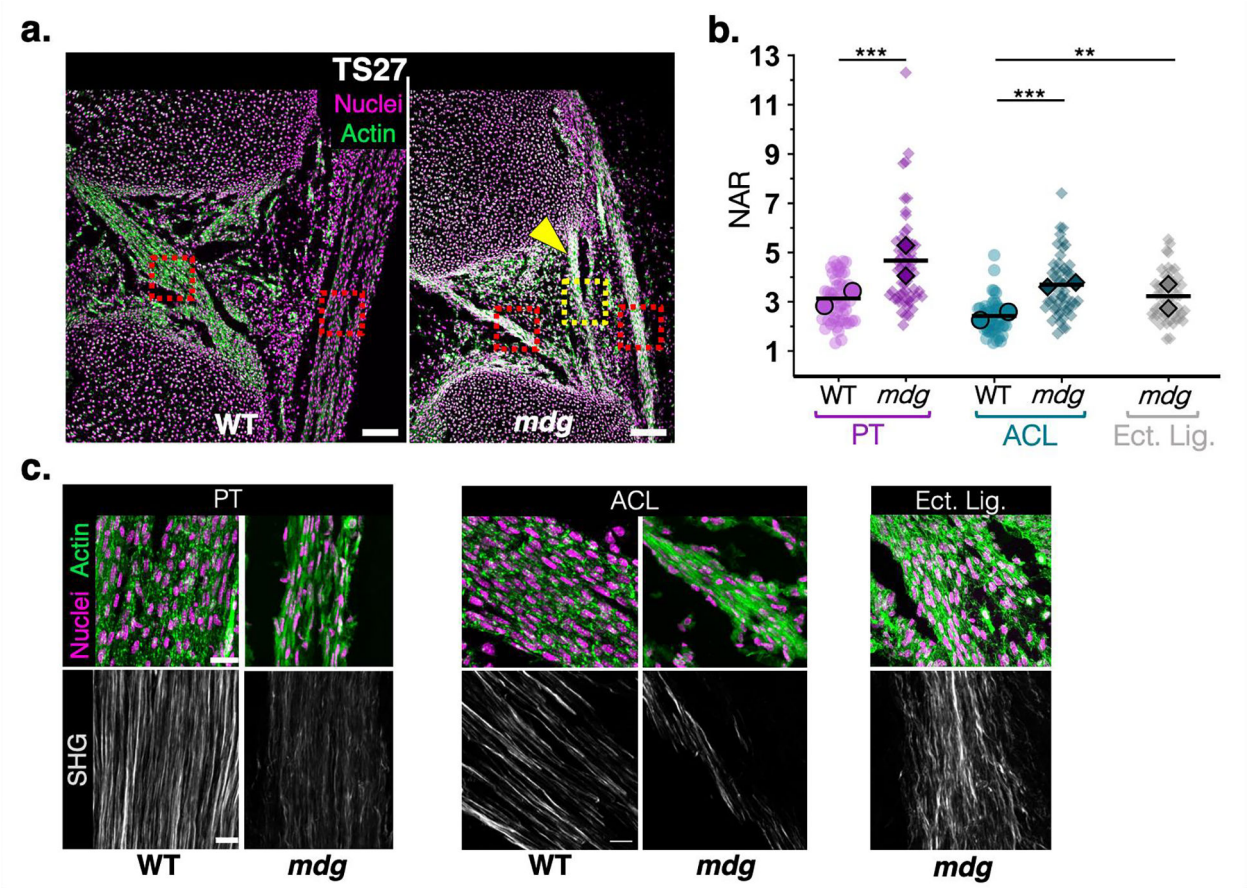

Figure 5: Abnormal nuclear and matrix structure of fibrous tissues in TS27 *mdg* knees.

A) Representative sagittal views of TS27 (E17.5) WT and *mdg* knee joints in the region of the ACL and the patellar tendon (PT). Sections were stained with phalloidin for actin (green) and a nuclear counterstain (magenta). Yellow arrowhead points to the ectopic ligament (Ect. Lig.). Red and yellow boxes denote regions imaged in c) (scale bar: 100μm). b) Nuclear aspect ratio (NAR) of resident cells in TS27 WT and *mdg* tissues: n>50 nuclei per group taken from 2 biological replicates (mean of each replicate indicated by black symbol). Kruskal-Wallis with Dunn's test for multiple comparisons. **: $p<0.001$; ***: $p<0.0001$. c) High magnification confocal maximum projections of actin and nuclei (top) or SHG signal (bottom) for WT and *mdg* tissues of the PT, ACL, and ectopic ligament (*mdg* mutant only) (scale bar: 20μm for top images, 10μm for bottom (SHG) images).

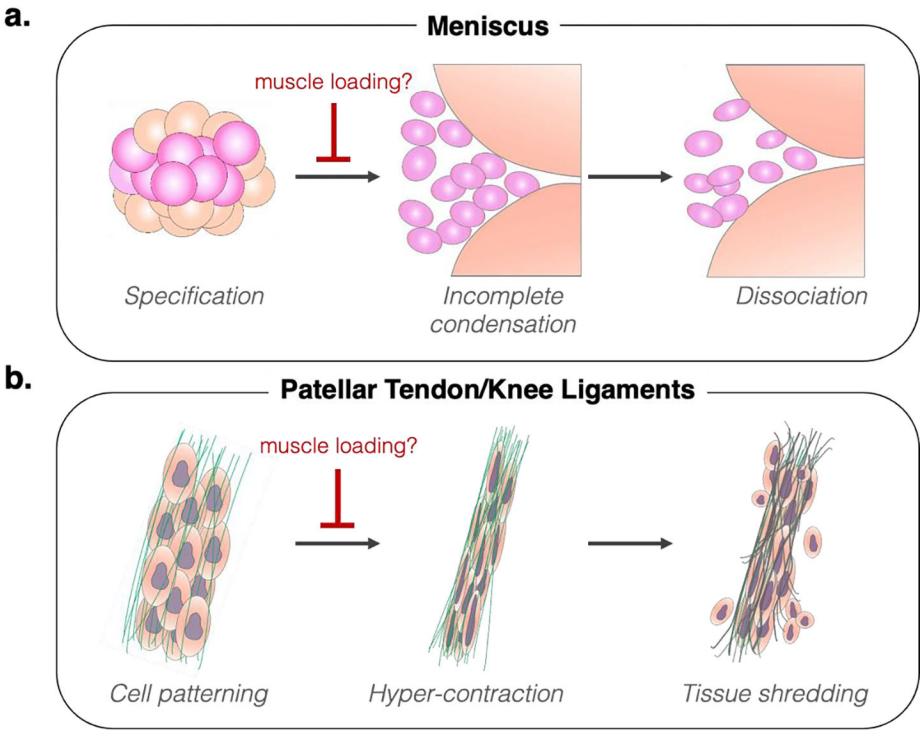

Figure 6: Impact of immobilization on knee joint fibrous tissue morphogenesis.

a) During meniscus formation, muscle loading plays a crucial role in maintaining cell condensation and permitting cell patterning. Without muscle contraction, condensation of meniscus precursor interzone cells is incomplete by the time of joint cavitation (TS24), and the formed cell mass fails to maintain a condensed state during subsequent growth, leading to dissociation of the tissue (TS27). **b)** For linear fibrous tissues of the knee (tendons and ligaments), loss of muscle loading does not generally impact the specification of these structures, except for the formation of the ectopic ligamentous tissue. However, lack of muscle contraction causes abnormal elongation of cells at the time of tissue formation (TS24), possibly indicating hypercontraction as an attempt to return to tensional homeostasis. This culminates in reduced tissue growth at later stages (TS27), which may be the result in tissue shredding due to concurrent increase of cell-generated forces and diminished material properties of the deposited extracellular material within the nascent tissue.